ISBN: 978-3-95450-214-1 ISSN: 2673-5490 doi:10.18429/JACoW-IPAC2021-THPAB049

MODELING THE MAGNETIC FIELD OF THE LCLS-I UNDULATOR FOR THz@PITZ*

M. Krasilnikov†, X.-K Li, A. Lueangaramwong, F. Mueller, F. Stephan, DESY, Zeuthen, Germany
M. Tischer, P. Vagin, DESY, Hamburg, Germany
A. Brachmann, H.-D. Nuhn, SLAC, Menlo Park, California, USA

Abstract

An accelerator-based THz source for pump-probe experiments at the European XFEL is under development at the Photo Injector Test Facility at DESY in Zeuthen (PITZ). For the proof-of-principle experiments an LCLS-I undulator is planned to be installed downstream of the PITZ accelerator. The fields of the undulator module 26 have been re-measured at DESY in Hamburg and the results are consistent with earlier SLAC measurements. A model for 3D field reconstruction based on the undulator magnetic measurements has been developed. It includes also a horizontal gradient of the vertical field. Tracking of the 17 MeV/c beam has revealed that the transverse gradient will lead to a significant off-axis trajectory in the horizontal plane. This offset has to be corrected with a steering coil, the design of which is also presented. The performance of the THz generation with the correction coil is discussed as well.

INTRODUCTION

The Photo Injector Test facility at DESY in Zeuthen (PITZ) is developing a prototype for an accelerator-based high power tunable THz source for pump and probe experiments at the European XFEL [1]. The SASE FEL is considered as the main option to generate THz pulses at PITZ using a high bunch charge (up to 4 nC) operation mode of the photo injector. An LCLS-I undulator (on loan from SLAC) [2] is considered to be used for proof-of-principles experiments on THz generation at PITZ (THz@PITZ). Two undulator modules were delivered to DESY in Hamburg, the magnetic field was remeasured showing good agreement with previous measurements at SLAC. The horizontal field gradient across the undulator was as well measured. The measured field profile including the horizontal gradient has been utilized to reconstruct a 3D magnetic field map for the beam transport through the undulator section. Tracking 17 MeV/c electron bunches through the modeled field revealed a fairly strong beam horizontal steering due to the horizontal gradient. A correction coil was designed to compensate for the effect of the horizontal field gradient. The simulation of THz SASE FEL with the correcting coil applied showed a good performance for the proof-of-principle experiments.

UNDULATOR FIELD MODELING

The LCLS-I undulator module is a 3.4-m-long permanent magnet planar hybrid structure with 113 periods of $\lambda_U = 30$ mm and a magnetic gap of 6.8 mm. The narrow vacuum chamber has a racetrack-like cross section, 11 mm wide and 5 mm high [2].

Magnetic Field Measurements

The axial magnetic field profile of the LCLS-I L143-112000-26 undulator module has been re-measured by the FS-US group at DESY in Hamburg. The measurements were performed using a Hall probe scan along the z-axis with a step of 0.5 mm. The results are shown in Fig. 1, the second field integral is in good agreement with similar measurements at SLAC before transportation of the undulator to DESY.

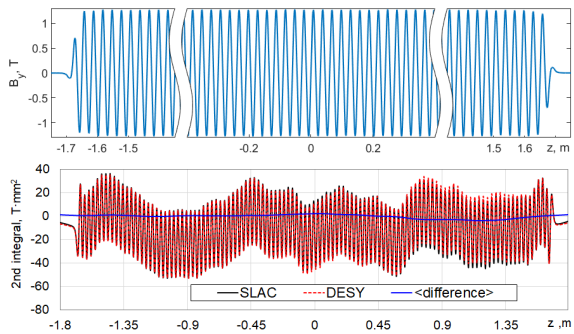

Figure 1: Top: Measured field profile $B_y(x = 0, y = 0, z)$ of the undulator module L143-112000-26. Bottom: The second field integrals: measured at SLAC, re-measured at DESY and the averaged difference. The center of the undulator corresponds to the point $z = 0$.

3D Field Map Reconstruction

Applying the Fourier transformation to the measured field profile $B_y(x = 0, y = 0, z)$ centered around $z = 0$ ($|z| \leq L/2$) the vertical component of the magnetic field reads as:

$$B_y(0,0,z) = \sum_{n=0}^{\infty} \left[a_n \cos(k_{zn} z) + b_n \sin(k_{zn} z) \right], \quad (1)$$

where $L = N_U \lambda_U$ is the undulator effective length and $k_{zn} = 2\pi n/L$ is the wavenumber of the n-th Fourier harmonic $\{a_n, b_n\}$. The specific shape of the field profile, including the spectral content of the regular periods, the end poles and the slope of strength, requires that a sufficiently large number of N_h harmonics must be taken into account to reproduce the measured field profile with sufficient accuracy. Proper centering and accurate processing of the measured field profile yields vanishing first and second field

* This work was supported by the European XFEL research and development program
† mikhail.krasilnikov@desy.de

ISBN: 978-3-95450-214-1 ISSN: 2673-5490 doi:10.18429/JACoW-IPAC2021-THPAB049

integrals. This corresponds to the conditions $a_n \approx 0$ and $\sum_{n=1}^{\infty}[(-1)^n b_n/n] \approx 0$ for the first and second integrals, respectively. The optimization resulted in $L = 120\lambda_U$ (despite the fact that nominally the undulator contains only 113 periods) and $N_h = 17$ - the harmonic number of the fundamental wavelength λ_U. This corresponds to the first 2040 ($= N_U \cdot N_h$) terms of the series in Eq. (1) taken into account. The Fourier spectrum and the field profile reconstructed from it are shown in Fig. 2 (left plot).

According to the original design the magnets are slightly canted with a 4.5-mrad opening angle [3]. This results in a horizontal gradient of the undulator field (Fig. 2, right plot). Both fits in this plot have the same linear slope $\alpha = -7.481 \cdot 10^{-4}$ T/mm. This coefficient was used to implement the horizontal gradient in the 3D field model.

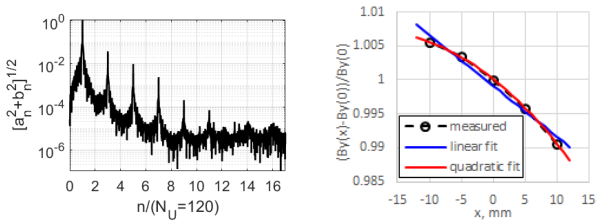

Figure 2: Left: Fourier spectrum Eq. (1) of the measured field. Right: measured horizontal gradient, blue line - a linear fit: $0.9991 - 7.481 \cdot 10^{-4} \cdot x$, red curve - a quadratic fit: $1.0001 - 7.481 \cdot 10^{-4} \cdot x - 2.025 \cdot 10^{-5} \cdot x^2$.

The reconstructed field map based on the magnetic scalar potential can be written as:

$$\chi(x,y,z) = -\frac{\cosh[k_x(x_0+x)]}{\cosh[k_x x_0]} \times \times \sum_{n=0}^{N_h N_U} \left([a_n \cos(k_{zn} z) + b_n \sin(k_{zn} z)] \cdot \frac{\sinh(k_{yn} y)}{k_{yn}} \right), \quad (2)$$

where the vertical wave number $k_{yn} = \sqrt{k_{zn}^2 - k_x^2}$, the horizontal wave number k_x can be obtained from the equation $k_x \cdot \tan[k_x x_0] = \alpha$ and the parameter $x_0 \approx 1.33$ m is calculated from geometric considerations (the undulator gap 6 mm and opening angle 4.5-mrad). Based on these considerations the horizontal wave number is calculated as $k_x \approx 0.916\,\mathrm{m}^{-1}$. All field components can be found from Eq. (2) by applying the gradient $\vec{B} = -\left\{\frac{\partial\chi}{\partial x}, \frac{\partial\chi}{\partial y}, \frac{\partial\chi}{\partial z}\right\}$. The 3D magnetic field map of the undulator calculated in this way, including the fringe fields and the horizontal gradient, can be applied to simulate the beam dynamics and the THz pulse generation.

BEAM DYNAMICS IN UNDULATOR

Previous simulations [4] with different codes for the case without the horizontal undulator gradient showed that the trajectory of the reference particle regularly wiggles around the axis of the vacuum chamber in the horizontal plane and coincides well with this axis in the vertical plane. Reference particle tracking with the ASTRA [5] using the 3D horizontal gradient undulator map from Eq. (2) was performed for a mean beam momentum of 17 MeV/c. This revealed a strong horizontal steering of the reference particle due to the accumulated difference in the left and right arcs of each oscillations in the horizontal plane (Fig. 3). The parallel on-axis injection of the reference particle into the undulator (black curve) results in a strong 25 mm beam offset at the undulator exit. Taking into account the finite width of the vacuum chamber of the undulator, this corresponds to the loss of the reference particle near the center of the undulator. The attempt to compensate for this influence of the horizontal gradient by the initial beam angle (blue curve) leads to the fact that the reference particle is centered at the exit of the undulator, but the reference particle touches the border of the vacuum chamber inside the undulator. This corresponds to significant loss of particles in the highly charged electron beam during its transportation through the undulator.

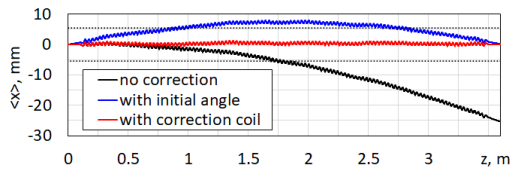

Figure 3: Reference particle trajectories in the undulator with a horizontal gradient: normal injection at the undulator entrance (black curve), initial horizontal angle for the horizontal gradient compensation (blue curve) and compensated by correction coil (red curve). The vacuum chamber border is shown by dotted line.

Correction Coil

To compensate for the effect of the horizontal gradient on the beam path, a correction coil (Fig. 4, left) was developed using CST EM Studio [6]. For a more realistic simulation, the magnetized parts of the undulator were included in the calculations of the fields from the four wires along the vacuum chamber according to the available space in the undulator. The right picture in this figure illustrates the technical implementation of this coil, including the very tight spatial constraints in the undulator near the vacuum chamber.

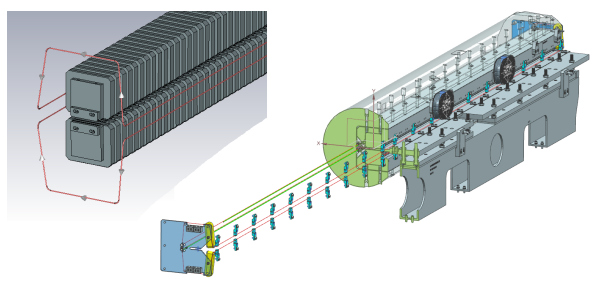

Figure 4: Left: Design of the compensation coil with CST EM Studio, including permanent magnets and iron insertions of the undulator. Right: Technical realization of the correction coil (red lines).

ISBN: 978-3-95450-214-1 ISSN: 2673-5490 doi:10.18429/JACoW-IPAC2021-THPAB049

The coil field components are shown in Fig. 5. The ripple in the left graph corresponds to the periodic structure of the magnetized parts, while the horizontal profile of B_y is fairly flat within the region of the vacuum chamber ($\pm$5.5 mm). A 3D magnetic field of the correction coil combined with the field map of the LCLS-I undulator with a horizontal gradient has been used for beam dynamics simulations. By tuning of the coil current it was possible to bring the reference particle onto the axis along entire undulator (red curve in Fig. 3).

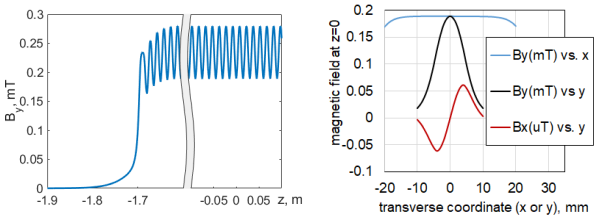

Figure 5: Magnetic field of the correction coil. Left: $B_y(z)$ in mT along the undulator axis ($z = 0$ corresponds to the middle of the undulator). Right: $B_y(x, y = 0, z = 0)$ and $B_y(x = 0, y, z = 0)$ in mT and $B_x(x = 0, y, z = 0)$ in µT.

THz SASE FEL SIMULATIONS

To study the effect of the horizontal gradient of the undulator compensated by the correction coil on the performance of the THz SASE FEL, the corresponding ASTRA [5] and PIC-code WARP [7] simulations were performed. Electron bunches with an average beam momentum of 17 MeV/c, a charge of 4 nC, and a flattop temporal profile with ~22 ps FWHM were matched to the LCLS-I undulator. As a reference case, a simulation with a 3D field map without a horizontal gradient was performed. The coil current (peak magnetic field) was carefully adjusted to minimize the deviation of the horizontal beam trajectory from the longitudinal axis. This resulted in an optimum value $\max\left[B_y^{coil}(0,0,z)\right] \approx 0.279$ mT, the corresponding horizontal trajectory is shown by the red curve in Fig. 6 (left graph) compared to the reference case (black curve). The right plot of Fig. 6 shows the rms transverse beam sizes along the undulator compared to the reference case. The comparison shows that it is possible to compensate well for the influence of the horizontal gradient of the undulator on the beam trajectory and envelope with a well-tuned correction coil.

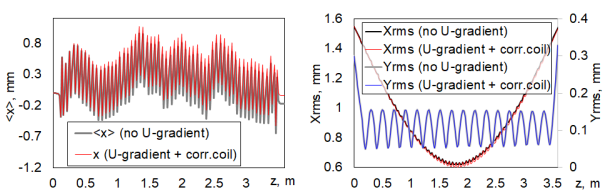

Figure 6: Left: Horizontal trajectory of the reference particle for the cases without and with the gradient of the undulator compensated by the correction coil. Right: Horizontal and vertical rms sizes of the electron beam along the undulator.

The results of the SASE FEL THz simulation for the case without and with the horizontal gradient of the undulator, as well as taking into account the compensation of the gradient by the correction coil, are shown in Fig. 7 (left plot). Uncompensated trajectories (the same color code as in Fig. 3) result in a significant drop in the output THz pulse energy. For both cases, without gradient and with compensated gradient,the output THz pulse energy ~0.6 mJ for an average radiation wavelength of 100 µm was simulated. This corresponds to the recovery of the effective overlap of the generated SASE radiation with the trajectories of the particles inside the undulator. These WARP simulations were performed assuming a narrow vacuum chamber by setting ideal electrically conductive boundary conditions for the corresponding rectangular waveguide. It should be noted that the simulated power density distributions of THz radiation at the output of the undulator for both of the above cases are similar. An example of the simulated power density distribution for the case with a horizontal field gradient of the undulator and a correction coil applied is shown in the right plot of Fig. 7. This gives us confidence that the proposed compensation of the horizontal field gradient of the undulator with the developed correction coil should be efficient.

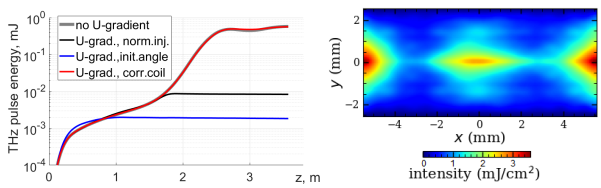

Figure 7: Left: Simulated THz energy of the SASE FEL pulse along the undulator for the cases without and with the undulator field gradient compensated by the correction coil. Right: Transverse distribution of THz power density at the output of the undulator for the case with the undulator field gradient compensated by the correction coil. The rectangular frame corresponds to the border of the vacuum chamber.

CONCLUSION

The LCLS-I undulator L143-112000-26 is planned to be installed downstream of the PITZ accelerator for the proof-of-principle experiments on the accelerator-based THz source for pump-probe experiments at the European XFEL. The undulator field re-measured at DESY is in good agreement with previous measurements at SLAC. A model was implemented for 3D field reconstruction based on magnetic measurements, including the horizontal field gradient. Tracking the beam with the modeled field revealed a significant horizontal offset of the beam, which cannot be compensated by the initial beam angle. A correction coil was developed to compensate for this effect. Beam dynamics simulations showed the possibility of almost complete compensation of the undulator field horizontal gradient effect with the correction coil for both the beam trajectory and envelope, as well as for the radiation performance of the THz SASE FEL.

ISBN: 978-3-95450-214-1 ISSN: 2673-5490 doi:10.18429/JACoW-IPAC2021-THPAB049

REFERENCES

[1] M. Krasilnikov, F. Stephan, E. Schneidmiller, and M. V. Yurkov, "Tunable IR/THz Source for Pump Probe Experiments at the European XFEL", in *Proc. 34th Int. Free Electron Laser Conf. (FEL'12)*, Nara, Japan, Aug. 2012, paper WEPD55, pp. 503–506.

[2] E. Trakhtenberg *et al.*, "Undulator for the LCLS project—from the prototype to the full-scale manufacturing", *Nucl. Instr. Meth. A*, vol. 543, pp. 42-46, 2005. doi:10.1016/j.nima.2005.01.110

[3] G. Pile *et al.*, "Design and Construction of the Linac Coherent Light Source (LCLS) Undulator System", in *Proc. 30th Int. Free Electron Laser Conf. (FEL'08)*, Gyeongju, Korea, Aug. 2008, paper THAAU01, pp. 460–466.

[4] M. Krasilnikov, P. Boonpornprasert, H.-D. Nuhn, E. Schneidmiller, F. Stephan, and M. V. Yurkov, "Start-to-End Simulations of THz SASE FEL Proof-of-Principle Experiment at PITZ", in *Proc. 13th International Computational Accelerator Physics Conference (ICAP'18)*, Key West, Florida, USA, Oct. 2018, pp. 246–252. doi:10.18429/JACoW-ICAP2018-TUPAF23

[5] K. Flöttmann, A Space Charge Tracking Algorithm (ASTRA), http://www.desy.de/~mpyflo/.

[6] Computer Simulation Technology, http://www.cst.com/.

[7] J.-L. Vay, C. G. R. Geddes, E. Esarey, C. B. Schroeder, W. P. Leemans, E. Cormier-Michel, and D. P. Grote, "Modeling of 10 GeV-1 TeV laser-plasma accelerators using Lorentz boosted simulations", *Physics of Plasmas*, vol. 18, p. 123103, 2011. doi:10.1063/1.3663841